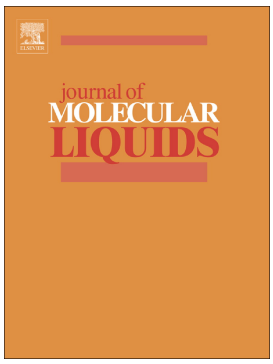


# Insights on the mixtures of imidazolium based ionic liquids with molecular solvents

A. Gutiérrez, M. Atilhan, R. Alcalde, J.L. Trenzado, S. Aparicio

PII: S0167-7322(17)34954-1
DOI: https://doi.org/10.1016/j.molliq.2018.01.167
Reference: MOLLIQ 8621

To appear in: *Journal of Molecular Liquids*

Received date: 17 October 2017
Revised date: 29 December 2017
Accepted date: 28 January 2018

Please cite this article as: A. Gutiérrez, M. Atilhan, R. Alcalde, J.L. Trenzado, S. Aparicio , Insights on the mixtures of imidazolium based ionic liquids with molecular solvents. The address for the corresponding author was captured as affiliation for all authors. Please check if appropriate. Molliq(2017), https://doi.org/10.1016/j.molliq.2018.01.167

# Insights on the Mixtures of Imidazolium Based Ionic Liquids with Molecular Solvents

A. Gutiérrez,[a] M. Atilhan,[b,c] R. Alcalde,[a] J. L. Trenzado,[*d] S. Aparicio[*a]

[a] Department of Chemistry, University of Burgos, 09001 Burgos, Spain

[b] Department of Chemical Engineering, Texas A&M University at Qatar, Doha, Qatar

[c] Gas and Fuels Research Center, Texas A&M University, College Station, TX, USA

[d] Departamento de Física, Universidad de Las Palmas de Gran Canaria, 35017 Las Palmas G.C., Spain

[*]Corresponding authors: jtrenzado@dfis.ulpgc.es (J. L. T.), sapar@ubu.es (S. A.)

**ABSTRACT:** The properties of ionic liquid (1-ethyl-3-methylimidazolium $BF_4$ and 1-butyl-3-methylimidazolium $BF_4$) + solvents (water, ethylene glycol or dimethylformamide) mixtures are studied in the full composition range as a function of mixture composition and temperature. These mixed fluids are characterized by selected physical properties and microscopic studies using density functional theory and molecular dynamics simulations. The reported results showed large non-ideal mixtures, which are caused by strong anion ($BF_4$) – molecular solvent hydrogen bonding. Likewise, the interactions of ions, evolves from anion-cation pairs solvated by molecular solvents, for mixtures rich in molecular solvent, to large ionic aggregates for ionic liquid rich mixtures separated by a transitional composition regime. The large non-linearity of the evolution of microscopic properties with mixture composition is the origin of macroscopic thermodynamic deviations from ideality.

**Keywords:** ionic liquid mixtures, molecular solvents, water, hydrogen bonding, simulation.

## 1. Introduction

Ionic liquids (ILs) are formed by ions with molecular characteristics such as bulky and asymmetric structures, delocalized charge, low charge density, presence of nonpolar alkylic chains and a proposed dual ionic and organic nature, which are the reason of their low melting temperature due to their effect on microscopic level features and intermolecular interactions [1-3]. These characteristics determine the properties and structure of pure ILs but also have a large effect when mixing with molecular solvents (MSs) [4-7]. Intermolecular forces between ILs and MSs are largely complex [810], even with the appearance of competition effects between the involved ions and molecules [11], because of their dependence on the protic or aprotic, polar or apolar, or hydrogen bonding ability of the MSs, and show remarkable changes with mixture composition, pressure and temperature [12-15]. These mechanisms of ILs-MSs interactions determine the macroscopic physicochemical properties of mixed fluids [1618], and thus, their possible application for several technologies at industrial level [1921]. This is of great relevance because many ILs have physicochemical properties such as high viscosity that are highly unsuitable for bulk scale applications [22,23], and thus these properties can be tailored not only by the selection of suitable ions but also by mixing with MSs [2426] at concentrations in which the desired properties and features of the ILs are maintained [2731]. Likewise, the limited solubility of relevant solutes in ILs may be enhanced by mixing ILs with suitable cosolvents [3234], and mechanism of chemical reactions and reaction rates can be controlled through the use of tailored ILs+MSs mixtures [35]. Therefore, developing ILs+MSs mixture would extend the number of possible ILs – based fluids for any required technology allowing a better control of ILs drawbacks.

The ILs+MSs based large platform for developing suitable solvents for many technologies requires the development of structure-property relationships, which allow to carry out *in silico* designs and selection of the most suitable molecular combinations according to the requirements, since pure experimental approach is not practical and feasible when the number of possible options are considered. On the other hand, the development of structure – property relationships requires the knowledge of intermolecular forces (MS-MS, MS-IL and IL-MS), fluids' structuring at the molecular level, and their evolution with mixture composition [46], and their relationship with macroscopic fluids

behaviour [36,37] Considering the large number of possible ILs and MSs, a systematic approach should be developed to infer the molecular features controlling the properties of mixed fluids as a function of molecular structures and chemical functionalities of the involved molecules. Literature studies have been reported for ILs + MSs considering many different types of MSs. Mixtures that involve water have attracted great attention because of the large effects of water on physicochemical properties of solutions [38], especially on the dynamic properties such as viscosity [39], the appearance of remarkable microscopic features such as water nanocluster formation [40], formation of nanodomains or nanoconfinement [41], or large changes in the extension of hydrogen bonding with mixture composition [42]. Likewise, many studies characterizing mixtures containing other types of MSs, such as hydrocarbons [43], alcohols [44], dimethylsulfoxide [45], acetonitrile [46], or acetone [47], to mention some relevant MSs, have showed many relevant structural and macroscopic features.

The most remarkable features in ILs+MSs mixtures stands from the protic or aprotic character of both types of compounds, which control the evolution of hydrogen bonding upon mixing, and thus the most relevant microscopic features and macroscopic properties. Therefore, to develop a systematic approach for the characterization of ILs+MSs mixtures, protic MSs (water and ethylene glycol (EG)) together with dimethylformamide (DMF), as representative of aprotic MSs were selected and mixed with alkylimidazolium – based ILs (1-ethyl-3-methylimidazolium $BF_4$, [EMIM][$BF_4$], and 1-butyl-3-methylimidazolium $BF_4$, [BMIM][$BF_4$]). The considered MSs were selected as representatives of protic and aprotic MSs, considering largely different molecular functionalities and polarities to analyse a wide range of possible effects upon mixing with ILs. The studied imidazolium-based ILs were selected because the properties of these ILs in pure state have been widely analysed in the literature [4850], and thus, the effect of mixing with the considered MSs can be more accurately inferred. Selected thermophysical properties (density and dynamic viscosity) were measured as a function of mixture composition and temperature, allowing to calculate excess and mixing properties, which provide deviations from ideality as quantification of intermolecular interactions and changes upon mixing in comparison with pure fluids. Complimentary theoretical studies using both Density Functional Theory (DFT) and molecular dynamics (MD) simulations were carried out to obtain a microscopic view of

mixtures structuring and intermolecular forces, hydrogen bonding and their relationship with macroscopic behaviour.

# 2. Methods

### 2.1 Materials

The chemicals used along this work are described in Table S1 (Electronic Supplementary Information, ESI), they were used as received from commercials suppliers without further purification, maintained in darkness over freshly activated molecular sieves (4 nm, Union Carbide) and degassed by ultrasound before use. The purity of these chemicals was also inferred from the comparison of measured thermophysical properties and their comparison with literature Table S2 (ESI). ILs + MSs liquid mixtures were prepared by weighing (Mettler AE240 balance, ±0.01 mg). The analysis of all uncertainty factors led to mixtures mole fractions with ±0.00004 estimated uncertainty.

### 2.2 Thermophysical properties

Density ($\rho$) was measured using vibrating-tube densitometry (Anton-Paar DMA-60/602), with cell temperature measured to ± 0.01 K (CKT-100 thermometer, Anton-Paar). Densimeter calibration was carried out using water (Panreac Hiperpur-plus) and n-heptane (Fluka > 99.5%) as reference fluids [51,52]. Calculated uncertainties were ±0.00002 $g \cdot cm^{-3}$ and ± 0.003 $cm^3 \cdot mol^{-1}$ for density and excess molar volume, respectively.

Ubbelohde viscometers were used for measuring kinematic viscosities ($\nu$), Schott-Gerätte AVS 350 viscometer, with temperature controlled and measured to ±0.01 K. Viscometer calibration was carried out by the instrument manufacturer. The estimated uncertainty was 0.4 %.

Experimental density and viscosity data allowed the calculation of excess volume, $V^E$, and mixing viscosity ($\Delta\eta$), which were obtained as explained [53]. Mixing viscosity was calculated as considered in eq. (1):

$$\Delta\eta = \eta - x_{IL} \times \eta_{IL} - x_{MS} \times \eta_{MS} \quad (1)$$

Where $\eta$ stands for the viscosity of the liquid mixture, and $x_{IL}$, $\eta_{IL}$, $x_{MS}$, $\eta_{MS}$ for the mole fraction and viscosity of pure IL and MS.

### 2.3 Molecular Modelling

DFT calculations at B3LYP [54-56] functional with 6-311++G(d,p) basis set combined with Grimme's method (DFT-D3) [57], for treating dispersion corrections, were carried out using ORCA program [58]. Interaction energies, $\Delta E$, for the considered molecular clusters were calculated from the difference of the energy for the total cluster and the sum of the energies for the corresponding monomers, with counterpoise procedure for correcting Basis Set Superposition Error (BSSE) [59].

MD simulations were carried out using the MDynaMix v.5.2 program [60]. The forcefield parameterizations for the studied ions and MSs are reported in Table S3 (ESI). The systems used are reported in Table S4 (ESI). Packmol [61] program was used for building initial simulation boxes. Periodic boundary conditions were applied for all MD simulations. Simulation procedure was developed in two stages: i) equilibration (10 ns) followed by ii) production (10 ns) runs; all of them in the NPT ensemble at the selected temperature and 0.1 MPa. Pressure and temperature were controlled using the Nose–Hoover method. Ewald method [62] (15 Å for cut-off radius) was used for treating Coulombic interactions. Equations of motion were solved with the Tuckerman–Berne double time step algorithm [63] (1 and 0.1 fs for long and short time steps). Lorentz-Berthelot mixing rules were used for treating Lennard-Jones cross terms. The cutoff for truncation of Lennard-Jones interactions was 14 Å. No additional methods were used for handling the long-range corrections.

## 3. Results and discussion

The measured thermophysical properties (density and viscosity) together with derived $V^E$ and $\Delta\eta$ are reported in Tables S5 to S10 (ESI) and plotted as a function of mixtures composition (in the full composition range), temperature, type of IL and type of MS in Figs. S1 to S12 (ESI). The $V^E$ reported in Fig. 1a show positive values in the full composition range, i.e. expansion upon mixing, for mixtures of both [EMIM][$BF_4$] and [BMIM][$BF_4$] with water and EG in contrast with negative values for mixtures with DMF. Bahadur et al. [64] reviewed the literature information for aqueous mixtures of several families of ionic liquids, showing positive $V^E$ for [EMIM][$BF_4$] and [BMIM][$BF_4$] with values in the range of those reported in this work. The positive $V^E$ values for the studied IL + water mixtures are a consequence of the disrupting effect of water addition because water – IL hydrogen bonding is not strong

enough to balance the perturbation of anion-cation interactions, i.e. leading to an expansive effect to accommodate water molecules. Nevertheless, results reported in Fig. 1a show that $V^E$ decreases on going from [EMIM][$BF_4$] to [BMIM][$BF_4$] water mixtures, whereas Bahadur et al. [64] showed some literature data reporting the opposite effect. The decrease of expansive character upon increase of alkyl chain, i.e. evolving from [EMIM][$BF_4$] to [BMIM][$BF_4$] water mixtures, is confirmed in this work by MD simulations (discussed in following sections), and it is in agreement with results by Rilo et al. [65] and Taib et al. [66] This behavior can be justified by the presence of certain apolar domains in [BMIM][$BF_4$] [67] in comparison with the absence of these domains in [EMIM][$BF_4$], which are less perturbated by the presence of water molecules thus leading to lower expansion for [BMIM][$BF_4$] aqueous mixtures. Likewise, the negative molar volume that is observed for [BMIM][$BF_4$] and [EMIM][$BF_4$] with the mixtures of [DMF] could also be due to the reason of the limitation of rotational motion, when the [DMF] molecules are accommodated gaps within the ions and ion clusters. Yet, [DMF] can form hydrogen bonds with ILs and thus shrinking the intermolecular voids of the final IL + MS cluster. Excess partial molar volumes reported in Fig. 2 show positive values in the whole composition range both for the IL and water, which agrees with the disrupting effect of both molecules in the hydrogen bonding network of the second compound, even for highly diluted solutions of water in IL and of IL in water, for which the large positive values close to $x$ = 0 and $x$ = 1 show the competing effect of solute-solvent and solvent-solvent hydrogen bonding. The differences between the behaviour of [EMIM][$BF_4$] to [BMIM][$BF_4$] water mixtures are more remarked when Δη is considered, Fig. 1b; although both systems show negative Δη, with minima at roughly 2 IL : 1 water molar ratios, values are 4 times larger for [BMIM][$BF_4$] than for [EMIM][$BF_4$], in agreement with previous literature [68]. Negative Δη agrees with positive $V^E$, the presence of water molecules expanding the fluids favours the diffusion of molecules, thus decreasing viscosity because of the Einstein's relationship although rotational molecular movement of molecules should also be considered. The large differences in Δη for [EMIM][$BF_4$] to [BMIM][$BF_4$] water mixtures must be caused mainly by steric effects rising by the trend to develop apolar domains in [BMIM][$BF_4$] water mixtures, because the strength of the interactions of both ILs with water molecules is very similar as showed by DFT results (Table 1). The temperature effect for aqueous mixtures on the studied properties is showed in Figs. S1 and S7, ESI, and Fig. 3 for both ILs. Expansion upon mixing with water increases with increasing temperature

in an almost linear way following a parallel evolution for both ILs, but changes are minor in the studied temperature, Fig. 3a. Regarding temperature effect on Δη, Fig. 3b, a non-linear decrease with increasing temperature is inferred, which show that the large disrupting effect of water molecules is more remarkable at low temperatures, as show the very large Δη for [EMIM][$BF_4$] aqueous mixtures.

The properties of IL + EG mixtures reported in Figs. 1 to 2 are very similar to those for aqueous ones: expansion upon mixing accompanied by negative Δη, with the only difference that slightly larger expansions are obtained for [BMIM][$BF_4$] than for [EMIM][$BF_4$]. This can be justified considering that although the presence of two hydroxyl groups in EG should lead to hydrogen bonding with ions EG molecules should have strong tendency to self-associate, creating voids, and thus leading to expansion upon addition of EG molecules to ILs [69], Fig. 1a. The larger size of EG in comparison with water molecules leads to larger expansion with [BMIM][$BF_4$] because the formation of certain apolar domains hinders and the trend of EG self-association leads to a la larger expansive effect in comparison with smaller water molecules. The similar characteristics of EG-IL and water-IL hydrogen bonding are confirmed by the sign, shape and values of Δη, Fig. 1b, and the values of excess partial molar volumes, which are lower than those in water mixtures but with equal trends, Fig. 2. Regarding the effect of temperature, trends parallel to those in water are obtained both for $V^E$ and Δη, Fig. 3.

The behaviour of mixtures containing DMF are remarkably different to those for water or EG containing mixtures, but these differences are obtained for volumetric properties, which are larger (in absolute value) and negative for DMF-based mixtures (Figs. 1a, 2 and 3a) whereas the behaviour of Δη (Fig. 1b) is almost equal for both ILs. Yet, excess molar volume for water and EG containing mixtures show maxima at roughly equimolar concentrations, mixtures with DMF show minima at toughly 1 IL : 2 DMF molar ratios for $V^E$, which is highly surprising considering that DMF mixtures show minima for 2 IL : 1 DMF molar ratio for Δη, Fig. 1. It should be remarked that DMF may act only as hydrogen bonding acceptors in contrast with water or EG molecules, which can both accept or donate hydrogen bonds, therefore DMF cannot self-aggregate through hydrogen bonding but it can form hydrogen bonds with ILs. The poor trend of DMF molecules to self-associate but its ability to hydrogen bond with imidazolium based ILs [70] should be the reason of the large negative $V^E$ and partial molar volumes, i.e. upon mixing with ILs DMF molecules tend to

develop hydrogen bonding with ILs, thus decreasing void volume and leading to contraction upon mixing; this effect should be more relevant for DMF-rich mixtures, which would justify the minima in $V^E$ for 1 IL : 2 DMF molar ratios. Nevertheless, the characteristics of DMF – IL hydrogen bonding should be very like those for water and EG, as justified from DFT results, which leads to similar Δη values.

Although certain conclusions on microscopic structuring can be inferred form the studied macroscopic properties as discussed in previous paragraphs, more detailed insights can be inferred from theoretical studies using DFT and MD approaches. For the study of IL – MS short range interactions several model clusters were considered, in which four different positions (higher binding energy interaction sites) for MS molecules around anion-cation ionic pairs were analysed, Fig. S13 (ESI). For these DFT studies only IL pairs in which BF4 anion interacts with C2-H imidazolium site were considered because as previous studies [48,71-73] have showed this is the prevailing and lowest energy interaction position in both ILs. The reported low energy clusters show that MS molecules can interact with the ion pair without disrupting it, $BF_4$ – MS hydrogen bonding is developed with several possible orientations above the anion (positions P1 to P3 with very minor energetic differences, Table 1) and with very minor effects in binding energy when changing the type of MS molecule or increasing cation alkyl chain length. Likewise, interaction of the MS with imidazolium ring in positions P4 has remarkably lower energies than anion – MS interactions as in positions 1 to 3, i.e. considering that anion-cation pair is not disrupted by the presence of MS molecules, the prevailing interaction site would be the ones reported in positions 1 to 3 for anion – MS interactions over cation – MS ones. Therefore, short range interactions in the studied mixtures should be characterized by cation – anion pairs interacting through coulombic and in minor extension, weaker, hydrogen bonding interactions, which would remain paired even when the anion interacts with the corresponding MS.

Complex features rising from steric, size and shape effects of the involved molecules would determine the behaviour of the studied IL + MS liquid mixtures which are not captured by the reported DFT results and require simulations of bulk liquid phases by MD. The validation of MD results to obtain a realistic picture of the studied fluids was carried out by comparison of selected physicochemical properties with experimental data. Results in Figs. 4a and 4b show an excellent agreement between experimental and MD predicted density in the full composition range and for all the studied mixtures. Excess molar volume

was also predicted by MD, and although the prediction of this property by MD is difficult (because packing, steric and intermolecular forces, and their evolution with composition are involved) [74,75], an excellent qualitative and quantitative agreement is obtained, Figs. 4c and 4d; thus, the reported force field parameterization may give an accurate microscopic description of the fluids properties and structuring.

Considering the importance of dynamic properties for analysing the characteristics of IL + MS mixtures, self-diffusion coefficients (*D*) for cation, anion and MS were calculated from MD simulations and reported in Fig. 5 for the full composition ranges. These results show a non-linear behaviour of *D* as a function of mixture composition for the three types of molecules, especially for mixtures containing water and DMF molecules. Three regimes can be inferred from the composition evolution of *D* with mixture composition: i) region up to 0.25 IL mole fraction, with a steeped decrease of *D* from the values of pure MS, ii) region in the 0.25 – 0.50 range IL mole fraction, which seems to be a transitional region, and iii) region with IL mole fraction larger than 0.50, which seem to be dominated by IL. In these three regions, the ordering of *D* is DMF mixtures > water mixtures > EG mixtures. Likewise, *D*(cation) > *D*(anion) for all the studied ILs and MS. These results could be interpreted as fluids dominated by MS for region 1, with isolated ionic pairs (Fig. 6) solvated by MS molecules. Transitional region 2, in which the decrease of *D*(MS) in comparison with values in region 1, leading to values close to those of ions, show that MS molecules diffuse highly correlated with ions, thus the aggregation of ions should increase leading to larger clusters, hydrogen bonded to MS molecules. Region 3 would correspond to fluids dominated by large anion-cation clusters with MS dispersed in void spaces, thus with very low mobility. It should be remarked the very low *D* values for EG, Fig. 5c, which can be originated by the large self-association of this molecule because of the presence of two hydroxyl groups. Regarding the effect of MS on self-diffusion, DFT results in Table 1 showed similar strengths of interactions for all the studied MS molecules with ion pairs. Nevertheless, the low self-association of DMF molecules should lead to solvation spheres around ionic pairs (for DMF rich mixtures, region 1) with DMF molecules hydrogen bonded to isolated ionic pairs but with the remaining DMF molecules in these spheres interacting between them through weaker intermolecular interactions. Therefore, larger *D* values for DMF in comparison with water and specially EG is obtained. This would justify also the mobility of ions for region 1 compositions. As the mixtures are richer in IL, evolving to region 2 and 3, MS molecules are

dispersed in IL dominated structures, thus the role of MS – ion interactions prevails over MS – MS ones, and thus the $D$ values of the three MS approach between them, in agreement with a picture of MS monomers interacting, confined, in IL-dominated fluids, with similar MS – ion strength of interactions.

Structural features were analysed by using center-of-mass radial distribution functions (RDFs) for selected relevant molecular pairs. Regarding RDFs for cation-anion pairs, Fig. 6, it is characterized by two peaks with maxima at roughly 3.8 and 5.8 Å. These two peaks, correspond to two solvation shells around each ion, defined by the corresponding minima in RDFs, and their position does not change with dilution in the three studied MSs, which confirm that the effect of addition of MSs is the dilution of ionic pairs in the corresponding MSs. Nevertheless, it should be remarked that cation-anion RDFs peaks corresponding to DMF-containing solutions are narrower and more intense than for water or EG-containing solutions, which would indicate a stronger association of ions in DMF solutions. Likewise, the effect of alkyl chain length in imidazolium ring is almost negligible for the three studied MSs. The solvation numbers obtained from RDFs, Figs. 6g and 6h, show a non-linear trend with mixture composition, which on one side justifies the large non-ideality experimentally reported in Figs. 1 and 2, and on the other show agrees with the three regimes discussed for the behaviour of self-diffusion coefficients.

The arrangement of ion-MSs interactions is analysed by the corresponding RDFs in Figs. 7 (cation-MSs) and 8 (anion-MSs). The analysis of these two Figs. Show that all the studied MSs interacts preferently with $BF_4$ whereas interactions with alkylimidazolium cation are less important, in agreement with the cation-anion-MSs model, and the minor disrupting effect on the cation – anion interaction through the C2(H) site in imidazolium ring. RDFs peaks are remarkably narrower and more intense for water-containing solutions whereas those for EG and DMF solutions are wider and less intense. Likewise, whereas for water-solutions a second band is defined, vanishing with increasing IL concentration and corresponding to a second solvation shell around the anion, this band appears as a shoulder of the first peak for EG-solutions or is not defined for DMF-solutions, in agreement with more efficient interactions and solvation for water-containing solutions. The evolution of the corresponding solvation numbers for the first solvation shell of ion-MSs interactions also follow a non-linear trend, with steeped increments for low IL concentrations, especially for water containing solutions.

Self-aggregation of MSs is analysed in RDFs reported in Fig. 9. Water-water RDFs show the characteristic first and narrow peak corresponding to self-hydrogen bonding with a decrease in intensity upon increase of ILs mole fraction. The second solvation peak also vanished with increasing IL concentrations, these effects together with the evolution of the corresponding solvation numbers show that the size of water hydrogen bonding clusters decreases upon water dilution in ILs, and for IL rich solutions isolated water monomers are dispersed in IL dominated fluids, i.e. water hydrogen bonding vanishes upon dilution in both ILs. Regarding EG self-aggregation, EG hydrogen bonding is less intense than for water solutions (wider and less intense RDFs peaks) but solvation numbers are surprisingly larger for EG than for water, and the size of EG clusters decreases slower than for water upon dilution in ILs. This behaviour agrees with the low self-diffusion coefficients for EG-containing solutions reported in Fig. 5 and show a large trend of EG molecules to remain self-associated even for highly diluted solutions in ILs. This can be justified by a minor trend of EG molecules to interact with $BF_4$ anion in comparison with water, Fig. 8, probably by steric effects. Analogous results are reported for DMF – containing solutions, although DMF molecules cannot be self-hydrogen bonded, results in Fig. 9 show large DMF clustering like those in EG as showed by the evolution of solvation numbers.

The evolution of intermolecular interaction energies, $E_{inter}$, with mixture composition is reported in Fig. 10 for all the involved molecular pairs. Regarding $E_{inter}$ for cation-anion interactions, the evolution reported in Figs. 10a and 10b shows a parallel behaviour to RDFs in Fig. 6, the increase (in absolute value) of $E_{inter}$ with increasing ILs mole fraction is non-linear, confirming the evolution from isolated anion-cation ion pairs for MSs rich solutions to larger aggregated for IL rich solutions. Likewise, $E_{inter}$ are larger for water containing solutions than for those with EG or DMF, which shows that EG and DMF have a disruptive effect on anion-cation interactions, probably because of steric effects. For ion-MSs interactions, results in Fig. 10 confirms stronger anion-MS than cation-MS ones, in agreement with the cation-anion-MS model of interaction reported in previous sections, i.e. MSs molecules interacting directly with anion. Regarding MS-MS $E_{inter}$, a complex non-linear evolution is reported in Fig. 10, large values are obtained for EG-containing solutions at low IL concentration in agreement with the trend of EG molecules to remain self-associated, whereas DMF show the lowest $E_{inter}$ because it cannot develop self-hydrogen bonding. The

almost null $E_{inter}$ values for IL – rich solutions confirm that most of MSs molecules are in the form of monomers directly interacting with $BF_4$ anion.

The extension of hydrogen bonding was quantified and reported in Fig. 11. These results confirm that MSs are preferentially hydrogen bonded to $BF_4$ anion, whereas hydrogen bonding with cation has only certain relevance for IL rich solutions. Nevertheless, for DMF solutions the extension of hydrogen bonding is much lower than for water or EG. Regarding anion-cation hydrogen bonding, the reported results in Fig. 11 show the non-linear increase in aggregation numbers with IL concentration with similar behaviour for the three studied MSs. Finally, MS-MS self-hydrogen bonding is remarkably larger for water solutions, very minor in DMF ones, and intermediate for EG solutions, evolving in a non-linear way with increasing IL concentration and vanishing (i.e. leading to MS monomers) for IL rich solutions.

## 4. Conclusion

The combined experimental and computational study on alkylimidazolium-based ionic liquids mixed with selected molecular solvents allowed a characterization of their properties at both microscopic and macroscopic level. The large non-idealities from the thermodynamics viewpoint are inferred from the evolution of the developed intermolecular forces at the molecular level. Highly diluted solutions of ionic liquid in molecular solvent are characterized by ion pairs isolated and surrounded by the corresponding solvent whereas the size of anion-cation pairs increases in a non-linear way with increasing ionic liquid concentration, in such a way that isolated molecular solvent monomers are present for ionic liquid rich solutions. The mixtures are characterized by large self-diffusion coefficients for molecular solvent rich solutions, except for mixtures containing ethylene glycol. The analysis of hydrogen bonding and interaction energies show an interaction model in which molecular solvent molecules are hydrogen bonded with $BF_4$ anion with minor disruption of anion-cation interaction, mainly through the C2-H site in imidazolium ring. Then increase of alkyl chain in imidazolium ring from ethyl to butyl does not have any remarkable effect on mixture properties. The development of non-linear evolutions of all the studied properties with mixture composition, characterized by three well defined regions, stands on the molecular basis of the large non-ideal behaviour of all the studied solutions.

## Acknowledgement

This work was funded by Junta de Castilla y León (Spain, project BU324U14). We also acknowledge The Foundation of Supercomputing Center of Castile and León (FCSCL, Spain) for providing supercomputing facilities. The statements made herein are solely the responsibility of the authors.

## Electronic supplementary information

Table S1 (chemical used in this work); Table S2 (experimental properties of pure fluids and comparison with literature); Table S3 (force field parameterizations used along this work); Table S4 (description of systems used for molecular dynamics simulations); Tables S5 to S10 (experimental properties of studied mixed fluids); Figures S1 to S12 (plots of excess volume and mixing viscosity for the studied mixed fluids); Figure S13 (clusters structures optimized with DFT); Figure S14 (plots of mean square displacement).

## References

[1] R. Shi, Y. Wang, Scientific Reports 6 (2016) 19644.
[2] R. Hayes, G. G. Warr, R. Atkin, Chem. Rev. 115 (2015) 6357-6426.
[3] A. Podgorsek, J. Jacquemin, A. A. H. Pádua, M. F. Costa Gomes, Chem. Rev. 116 (2016) 6075-6106.
[4] B. Docampo-Alvarez, V. Gomez-Gonzalez, T. Mendez-Morales, J. Carrete, J. R. Rodríguez, O. Cabeza, L. J. Gallego, L. M. Varela, J. Chem. Phys. 140 (2014) 214502.
[5] O. Russina, A. Sferrazza, R. Cminiti, A. Triolo, J. Phys. Chem. Lett. 5 (2014) 1738-1742.
[6] V. V. Chaban, RSC Adv. 6 (2016) 8906-8912.
[7] M. H. Kowsari, L. Tohidifar, J. Phys. Chem. B 120 (2016) 10824-10838.
[8] H. K. Stassen, R. Ludwig, A. Wulf, J. Dupont, Chem. Eur. J. 21 (2015) 8324-8335.
[9] L. M. Varela, T. Méndez-Morales, J. Carrete, V. Gómez-González, B. Docampo-Álvarez, l. J. Gallego, O. Cabeza, O. Russina, J. Mol. Liq. 210 (2015) 178-188.
[10] J. E. S. J. Reid, R. J. Gammons, J. M. Slattery, A. J. Walker, S. Shimizu, J. Phys. Chem. B 121 (2017) 599-609.
[11] B. A. Marekha, O. N. Kalugin, M. Bria, T. Takamuku, S. Gadzuric, A. Idrissi, ChemPhysChem 18 (2017) 718-721.
[12] A. M. Smith, A. A. Lee, S. Perkin, Phys. Rev. Lett. 118 (2017) 096002.
[13] S. W. Coles, A. M. Smith, M. V. Fedorov, F. Hausen, S. Perkin, Faraday Discuss. 2017, DOI: 10.1039/C7FD00168A.
[14] S. Rathan, P. Bandlamudi, M. J. Cooney, G. L. Martin, K. M. Benjamin, Ind. Eng. Chem. Res. 56 (2017) 3040-3048.
[15] H. Montes-Campos, J. M. Otero-Mato, T. Méndez-Morales, E. López-Lago, O. Rusina, O. Cabeza, L. J. Gallego, L. M. Varela, J. Chem. Phys. 146 (2017) 124503.
[16] F. Ye, J. Zhu, K. Yu, R. Zhu, Y. Xu, J. Chen, L. Chen, J. Chem. Thermodyn. 97 (2016) 39-47.
[17] A. F. S. Santos, M. L. C. J. Moita, J. F. C. C. Silva, I. M. S. Lampreia, J. Chem. Thermodyn. 104 (2017) 118-127.
[18] A. Sharma, Y. Zhang, T. Gohndrone, S. Oh, J. F. Brennecke, M. J. McCready, E. J. Maginn, Chem. Eng. Sci. 159 (2017) 43-57.
[19] M. Ali, A. Sarkar, M. Tariq, A. Ali and S. Pandey, Green Chem. 9 (2007) 1252–1258.
[20] P. M. Mancini, G. G. Fortunato, C. G. Adam, L. R. Vottero, J. Phys. Org. Chem. 21 (2008) 87–95.

[21] G. G. Fortunato, P. M. Mancini, M. V. Bravo, C. G. Adam, J. Phys. Chem. B 114 (2010) 11804−11819.
[22] S. Aparicio, M. Atilhan, F. Karadas, Ind. Eng. Chem. Res. 49 (2010) 9580-9595.
[23] G. Yu, D. Zhao, L. Wen, S. Yang, X. Chen, AIChE J. 58 (2012) 2885-2899.
[24] J. Y. Wu, Y. P. Chen, C. S. Su, J. Sol. Chem. 44 (2015) 395-412.
[25] Q. Cao, X. Lu, X. Wu, Y. Guo, L. Xu, W. Fang, J. Chem. Eng. Data 60 (2015) 455-463.
[26] O. Ciocirlan, O. Croitoru, O. Iulian, J. Chem. Thermodyn. 101 (2016) 285-292.
[27] V. Ruiz, T. Huynh, S. R. Sivakhumar, A. G. Pandolfo, RSC Adv. 2 (2012) 5591-5598.
[28] A. M. Smith, A. A. Lee, S. Perkins, Phys. Rev. Lett. 118 (2017) 096002.
[29] V. Govinda, P. M. Reddy, P. Attri, P. Venkatesu, P. Venkateswarlu, J. Chem. Thermodyn. 58 (2013) 269−278.
[30] A. Ali, M. Ali, N. A. Malik, S. Uzair, A. B. Khan, J. Chem. Eng. Data 59 (2014) 1755-1765.
[31] J. M. Ardanson, E. Bordes, J. Devemy, F. Leroux, A. A. H. Pádua, M. F. Costa, Green Chem. 16 (2014) 2528-2538.
[32] S. R. P. Bandlamudi, M. J. Cooney, G. L. Martin, K. M. Benjamin, Ind. Eng. Chem. Res. 56 (2017) 3040-3048.
[33] A. Xu, Y. Zhang, Y. Zhao, J. Wang, Carbohyd. Polym. 92 (2013) 540-544.
[34] D. L. Minnick, R. A. Flores, M. R. DeStefano, A. M. Scurto, J. Phys. Chem. B 120 (2016) 7906-7919.
[35] S. T. Keaveney, T. L. Greaves, D. F. Kennedy, J. B. Harper, J. Phys. Chem. B 120 (2016) 12687-12699.
[36] M. Chen, R. Pendrill, G. Widmalm, J. W. Brady, J. Wohlert, J. Chem. Theory Comput. 10 (2014) 4465-4479.
[37] M. Tariq, K. Shimizu, J. M. S. S. Esperanca, J. N. Canongia-Lopes, L. P. N. Rebelo, Phys. Chem. Chem. Phys. 17 (2015) 13480-13494.
[38] Y. Kohno, H. Ohno, Chem. Commun. 48 (2012) 7119-7130.
[39] A. P. Singh, R. L. Gardas, S. Senapati, Soft Matter 13 (2017) 2348-2361.
[40] J. Gao, N. J. Wagner, Langmuir 32 (2016) 5078-5084.
[41] K. Saihara, Y. Yoshimura, S. Ohta, A. Shimizu, Scientific Reports 5 (2015) 10619.
[42] S. Cha, M. Ao, W. Sung, B. Moon, B. Ahlström, P. Johansson, Y. Ouchi, D. Kim, Phys. Chem. Chem. Phys. 16 (2014) 9591-9601.
[43] M. Liang, S. Khatun, E. W. Castner Jr, J. Chem. Phys. 142 (2015) 121101.
[44] W. Schroer, A. Triolo, O. Russina, J. Phys. Chem. B 120 (2016) 2638-2643.
[45] K. Fumino, V. Fossog, P. Stange, K. Wittler, W. Polet, R. Hempelmann, R. Ludwig, ChemPhysChem 15 (2014) 2604-2609.
[46] M. Bester-Rogac, A. Stoppa, R. Buchner, J. Phys. Chem. B 118 (2014) 1426-1435.
[47] E. Ruiz, v. r. Fero, J. Palomar, J. Ortega, J. Rodríguez, J. Phys. Chem. B 117 (2013) 7388-7398.
[48] J. A. Fournier, C. T. Wolke, C. J. Johnson, A. B. McCoy, M. A. Johnson, J. Chem. Phys. 142 (2015) 064306.
[49] V. Lesch, A. Heuer, C. Holm, J. Smiatek, ChemPhysChem 17 (2016) 387-394.
[50] C. Y. Son, J. G. McDaniel, J. R. Schmidt, Q. Cui, A. Yethiraj, J. Phys. Chem. B 120 (2016) 3560-3568.
[51] W. Wagner, A. Pru, J. Phys. Chem. Ref. Data 31 (2002) 387-535.
[52] E. W. Lemmon, M. L. Huber, M. McLinden, Reference Fluid, Thermodynamic, Transport Properties. NIST Standard Reference Database 23, version 9.0; The National Institute of Standards, Technology: Gaithersburg, MD, 2010.
[53] S. Aparicio, M. J. Davila, R. Alcalde, Energy Fuels 23 (2009) 1591−1602.
[54] C. Lee, W. Yang, R. G. Parr, Phys. Rev. B 37 (1988) 785-789.
[55] A. D. Becke, Phys. Rev. A 38 (1988) 3098-3100.
[56] A. D. Becke, J. Chem. Phys. 98 (1993) 5648 – 5652.
[57] S. Grimme, J. Antony, S. Ehrlich, H. A. Krieg, J. Chem. Phys. 132 (2010) 154104.
[58] F. Neese, WIREs Comput. Mol. Sci. 2 (2012) 73-78.
[59] S. Simon, M. Duran, J. Dannenberg, J. Chem. Phys. 105 (1996) 11024.
[60] A. P. Lyubartsev, A. Laaksonen, Comput. Phys. Commun. 128 (2000) 565-589.
[61] L. Martínez, R.,rade, E. G. Birgin, J. M. Martínez, J. Comput. Chem. 30 (2009) 2157-2164.
[62] U. L. Essmann, M. L. Perera, T. Berkowitz, H. Darden, H. Lee, L. G. Pedersen, J. Chem. Phys. 103 (1995) 8577-8593.
[63] M. Tuckerman, B. J. Berne, G. J. Martyna, J. Chem. Phys. 97 (1992) 1990-2001.
[64] I. Bahadur, T. M. Letcher, S. Singh, G. G. Redhi, P. Venkatesu, D. Ramjugernath, J. Chem. Thermodyn. 82 (2015) 34-46.
[65] E. Rilo, J. Pico, S. García-Garabal, L. M. Varela, O. Cabeza, Fluid Phase Equilibr. 285 (2009) 83-89.
[66] M. Taib, T. Murigesan, J. Chem. Eng. Data 57 (2012)120-126.
[67] M. Moreno, F. Catigliones, A. Mele, C. Pasqui, G. Raos, J. Phys. Chem. B 112 (2008) 7826-7836.

[68] Q. Zhou, L. S. Wang, H. P. Chen. J. Chem. Eng. Data 51 (2006) 905-908.
[69] T. Singh, A. Kumar, M. Kaur, g. Kaur, H. Kumar, J. Chem. Thermodyn. 41 (2009) 717-723.
[70] P. Attri, P. Madhusudan, P. Venkatesu, A. Kumar, T. Hofman, J. Phys. Chem. B 114 (2010) 6126-6133.
[71] S. A. Katsyubu, P. Dyson, E. E. Vandyukova, A. V. Chernova, A. Vidis, Helv. Chim. Acta 87 (2004) 2556-2565.
[72] R. Holomb, A. Martinelli, I. Albinsson, J. C.Lasségues, P. Johansson, P. Jacobson, J. Raman Spectrosc. 39 (2008) 793-805.
[73] T. Pal, R. Biswas, J. Phys. Chem. B 119 (2015) 15683-15695.
[74] B. Docampo-álvarez, V. Gómez-González, T. Méndez-Morales, J. R. Rodíguez, E. López-Lago, O. Cabeza, L. J. Gallego, L. M. Varela, Phys. Chem. Chem. Phys. 18 (2016) 23932-23943.
[75] U. Kapoor, J. K. Shah, Ind. Eng. Chem. Res. 55 (2016) 13132-13146.

**Table 1**

Counterpoise corrected binding energies, *ΔE*, for the reported clusters in the interacting positions P1 to P4 as reported in Figure S13 (Electronic Supplementary Information). *ΔE* is calculated as the difference between the energy of the cluster and the sum of those for the optimized monomers

| | Δ*E* kJ mol$^{-1}$ | Δ*E* kJ mol$^{-1}$ |
|---|---|---|
| | [EMIM][$BF_4$]+$H_2O$ | [BMIM+][$BF_4$]+$H_2O$ |
| P1 | -412.0 | -402.5 |
| P2 | -417.4 | -413.1 |
| P3 | -417.2 | -411.1 |
| P4 | -387.1 | -382.3 |
| | [EMIM][$BF_4$]+EG | [BMIM+][$BF_4$]+EG |
| P1 | -417.6 | -424.0 |
| P2 | -413.3 | -415.6 |
| P3 | -414.2 | -405.3 |
| P4 | -389.3 | -383.9 |
| | [EMIM][$BF_4$]+DMF | [BMIM+][$BF_4$]+DMF |
| P1 | -427.7 | -415.2 |
| P2 | -418.1 | -417.5 |
| P3 | -418.8 | -421.1 |
| P4 | -399.5 | -395.1 |

**Figure Captions**

**Fig. 1.** (a) excess volume, $V^E$, and (b) mixing viscosity, Δη, for the reported mixtures at 293.15 K. *x* stands for ionic liquid mole fraction.

**Fig. 2**. Excess partial molar volume of (a) ionic liquid, $V_{IL}^E$, and (b) molecular solvent (water, EG or DMF), $V_{MS}^E$, for the reported mixtures at 293.15 K. Values at $x = 0$ or $x = 1$ are the corresponding values at infinite dilution. *x* stands for ionic liquid mole fraction.

**Fig. 3.** Temperature effect on the minima or maxima of (a) excess volume, $V^E$, and (b) mixing viscosity, Δη, for the reported mixtures.

**Fig. 4**. Comparison between experimental (EXP) and predicted from molecular dynamics simulations (MD) density (ρ) and excess volume ($V^E$) in the reported mixtures at 293.15 K. *x* stands for ionic liquid mole fraction.

**Fig. 5.** Self-diffusion coefficients, *D*, in the reported mixtures at 293.15 K. *x* stands for ionic liquid mole fraction.

**Fig. 6.** Anion-cation centers-of-mass radial distribution functions, *g*(*r*), panels a to f, and the corresponding solvation numbers in the first solvation sphere, panels g and h (for [EMIM][$BF_4$] and [BMIM][$BF_4$] containing mixtures, respectively), in the reported mixtures at 293.15 K. *x* stands for ionic liquid mole fraction. Dashed lines in panels a to f show the distance for the first and second solvation shells, which are reported in panels g and h.

**Fig. 7.** Cation-molecular solvent center-of-mass radial distribution functions, *g*(*r*), panels a to f, and the corresponding solvation numbers in the second solvation sphere, panels g and h (for [EMIM][$BF_4$] and [BMIM][$BF_4$] containing mixtures, respectively), in the reported mixtures at 293.15 K. *x* stands for ionic liquid mole fraction. Dashed lines in panels a to f show the distance for the first and second solvation shells, which are reported in panels g and h.

**Fig. 8.** Anion-molecular solvent center-of-mass radial distribution functions, *g*(*r*), panels a to f, and the corresponding solvation numbers in the first solvation sphere, panels g and h (for [EMIM][$BF_4$] and [BMIM][$BF_4$] containing mixtures, respectively), in the reported mixtures at 293.15 K. *x* stands for ionic liquid mole fraction. Dashed lines in panels a to f show the distance for the first and second solvation shells, which are reported in panels g and h.

**Fig. 9.** Molecular solvent-molecular solvent center-of-mass radial distribution functions, $g(r)$, panels a to f, and the corresponding solvation numbers in the first solvation sphere, panels g and h (for [EMIM][$BF_4$] and [BMIM][$BF_4$] containing mixtures, respectively), in the reported mixtures at 293.15 K. *x* stands for ionic liquid mole fraction. Dashed lines in panels a to f show the distance for the first and second solvation shells, which are reported in panels g and h.

**Fig. 10.** Intermolecular interaction energy, $E_{inter}$ (sum of coulombic and Lennard-Jones contributions), for the reported molecular pairs, in the reported mixtures at 293.15 K. *x* stands for ionic liquid mole fraction. MS stands for molecular solvent (water, EG or DMF).

**Fig. 11.** Average number of hydrogen bonds, $N_H$, for the reported molecular pairs in the reported mixtures at 293.15 K. *x* stands for ionic liquid mole fraction. MS stands for molecular solvent (water, EG or DMF). The criterion used for defining hydrogen bonds was 3.5 Å and 60$^o$ for donor-acceptor distance and separation angle. The following sites were considered for calculating hydrogen bonds: (anion-cation) C2-H site in cation and F atoms in $BF_4$ anion; (anion - MS) F atoms in $BF_4$ anion and H atoms in water (water mixtures), or OH sites in EG (EG mixtures) or Hydrogen atoms in -CHO site of DMF (DMF mixtures); (cation-MS) C2-H (red lines) or C1-H (cyan lines) sites in cation and O atom in water (water mixtures) or O atoms in EG (EG mixtures) or O atoms in DMF DMF mixtures); (MS-MS) OH sites in water (water mixtures) or OH sites in EG (EG mixtures) or -CHO sites in DMF (DMF mixtures).

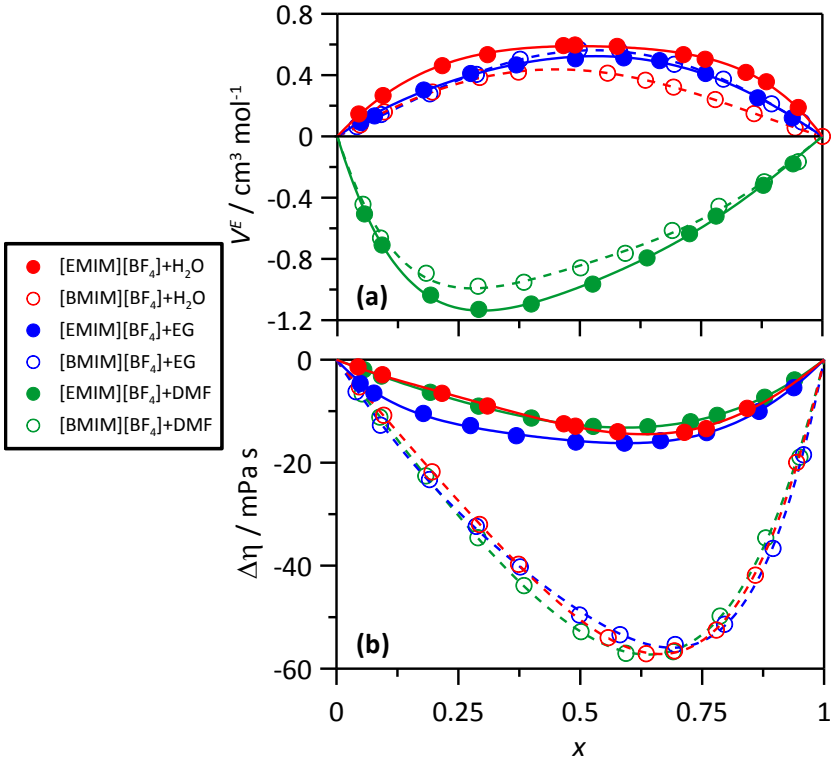


**Fig. 1.**

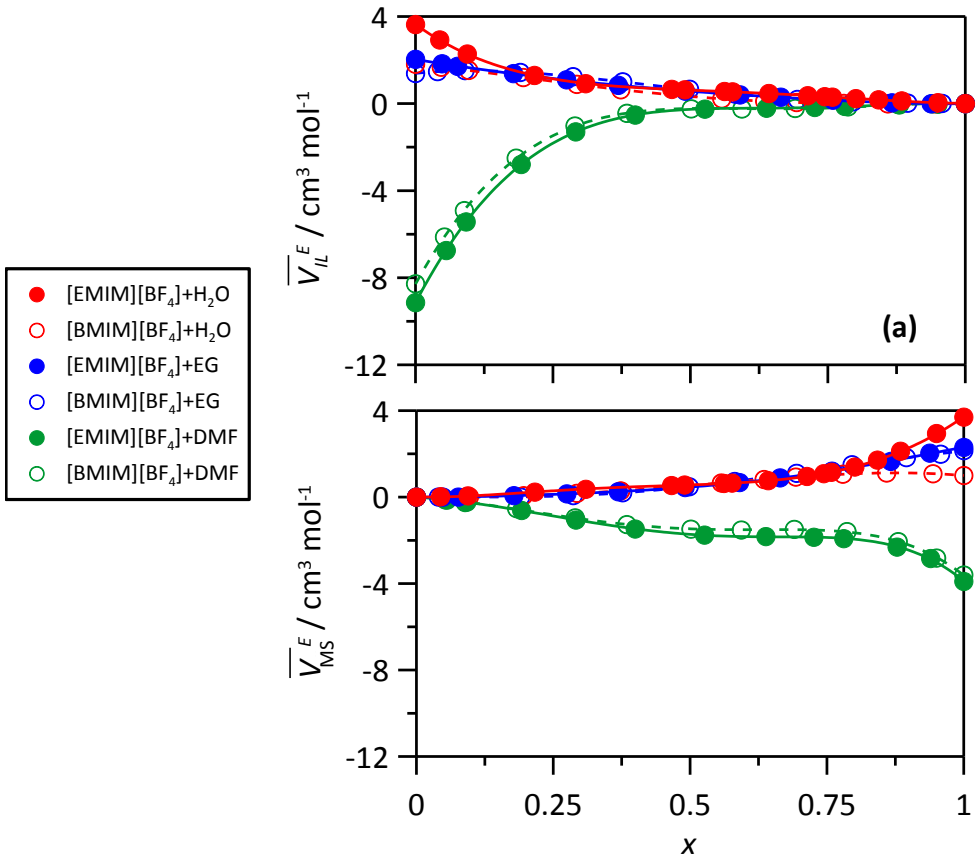


**Fig. 2.**

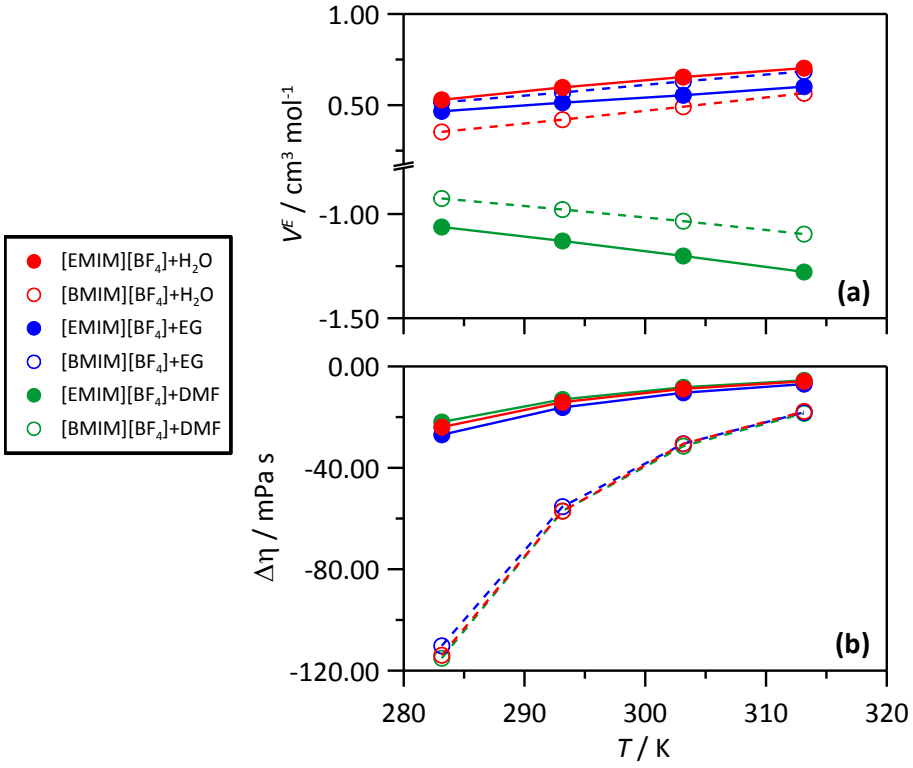


**Fig. 3.**

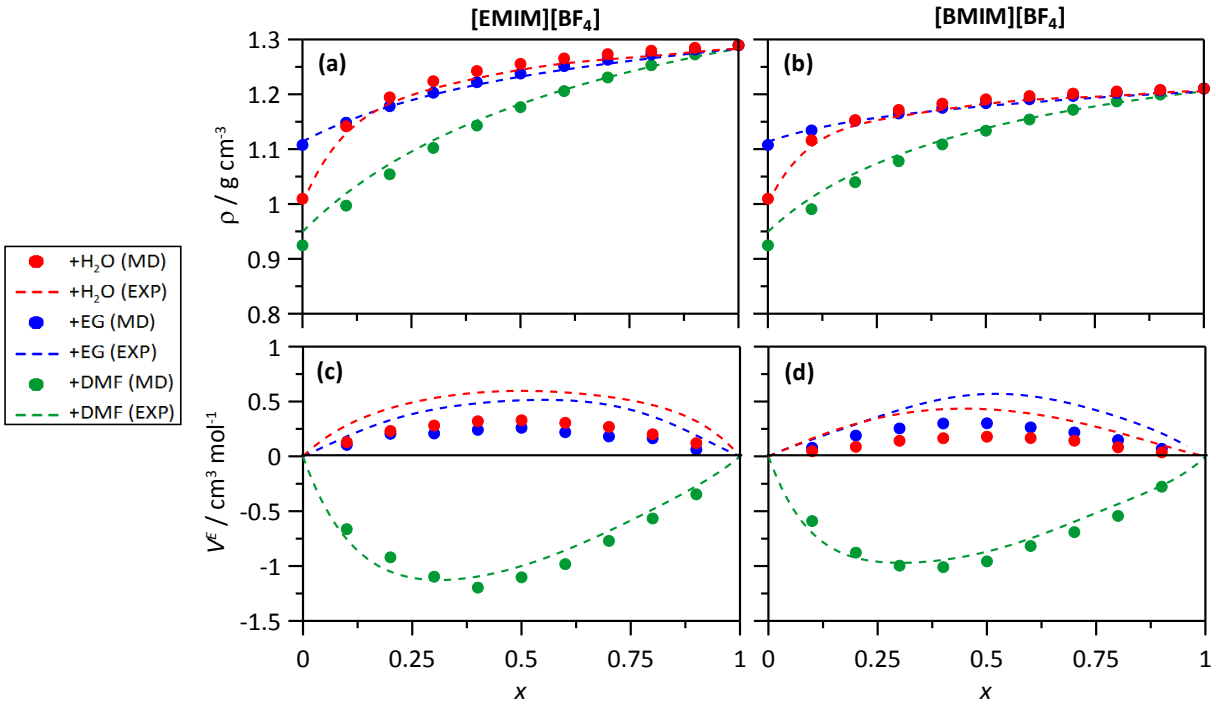


**Fig. 4.**

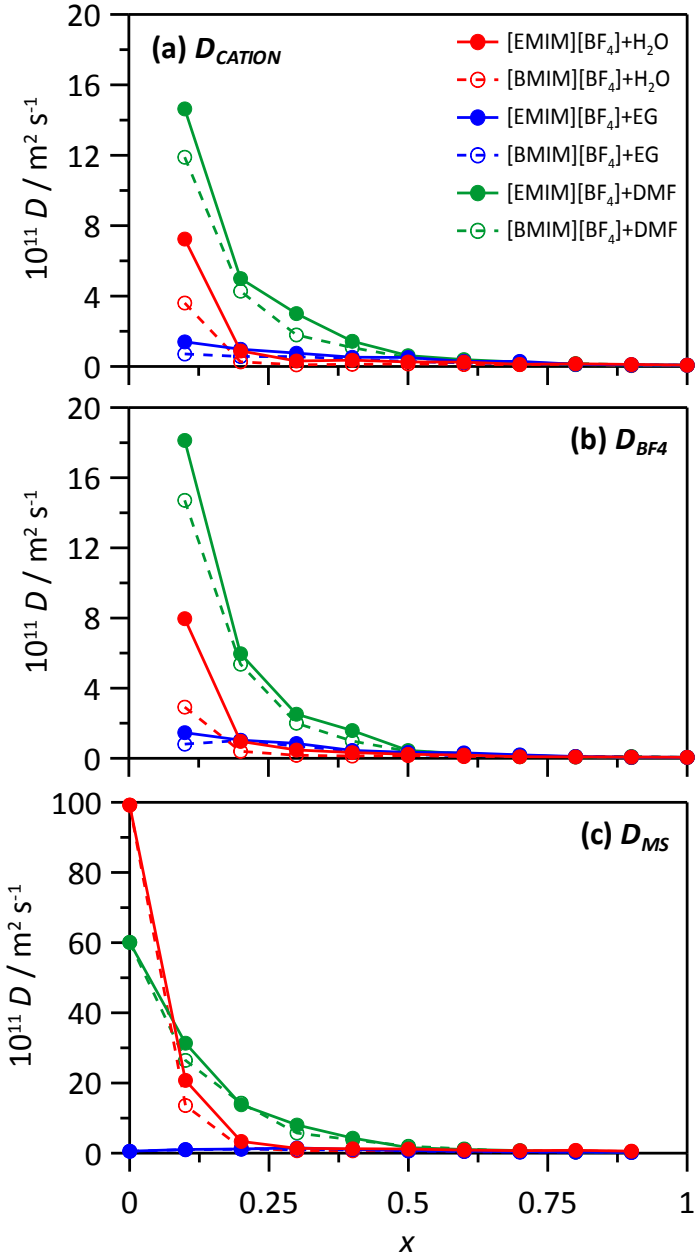


**Fig. 5.**

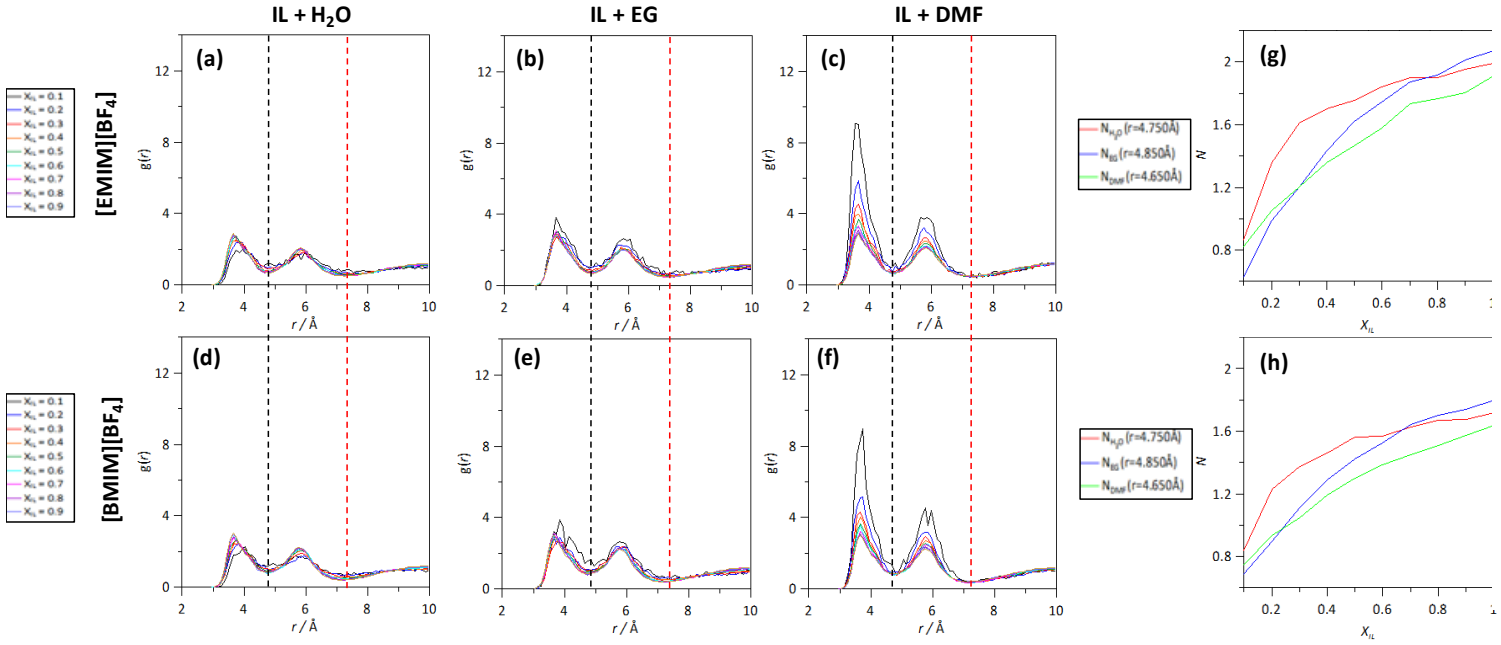


**Fig. 6.**

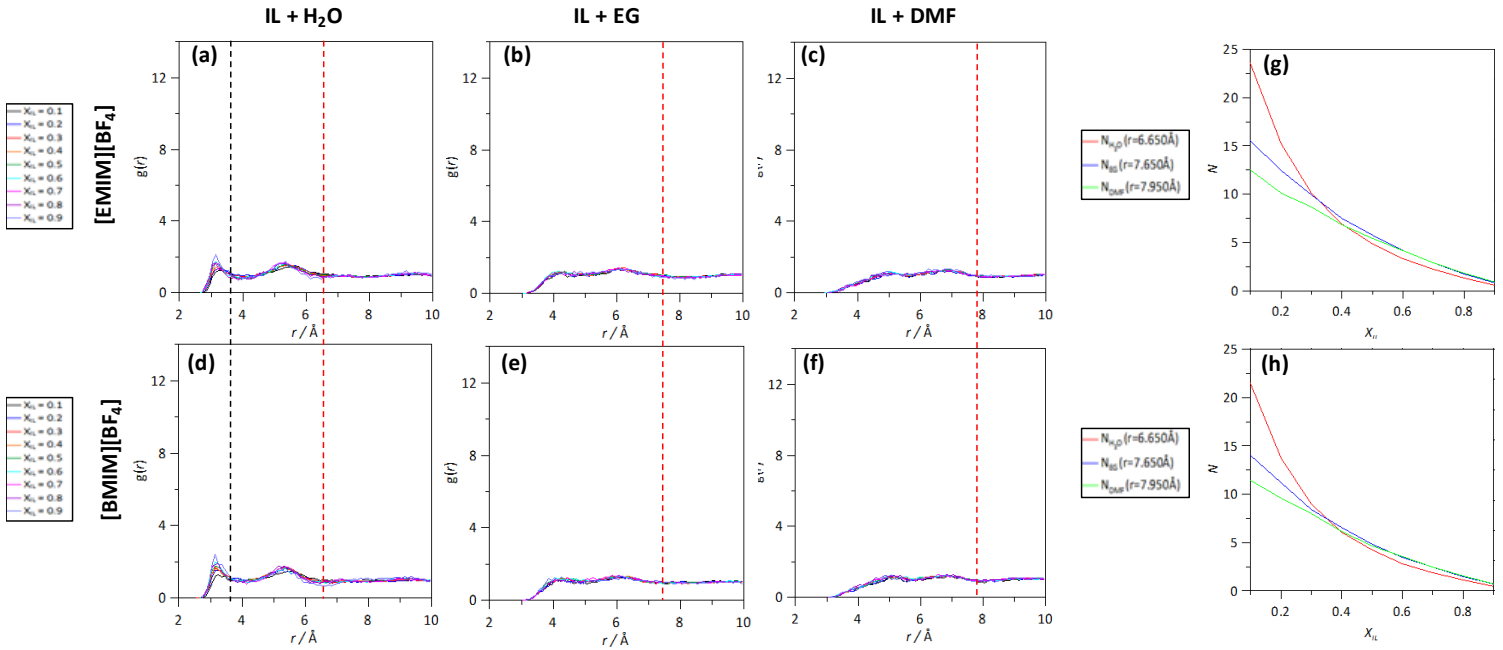


**Fig. 7.**

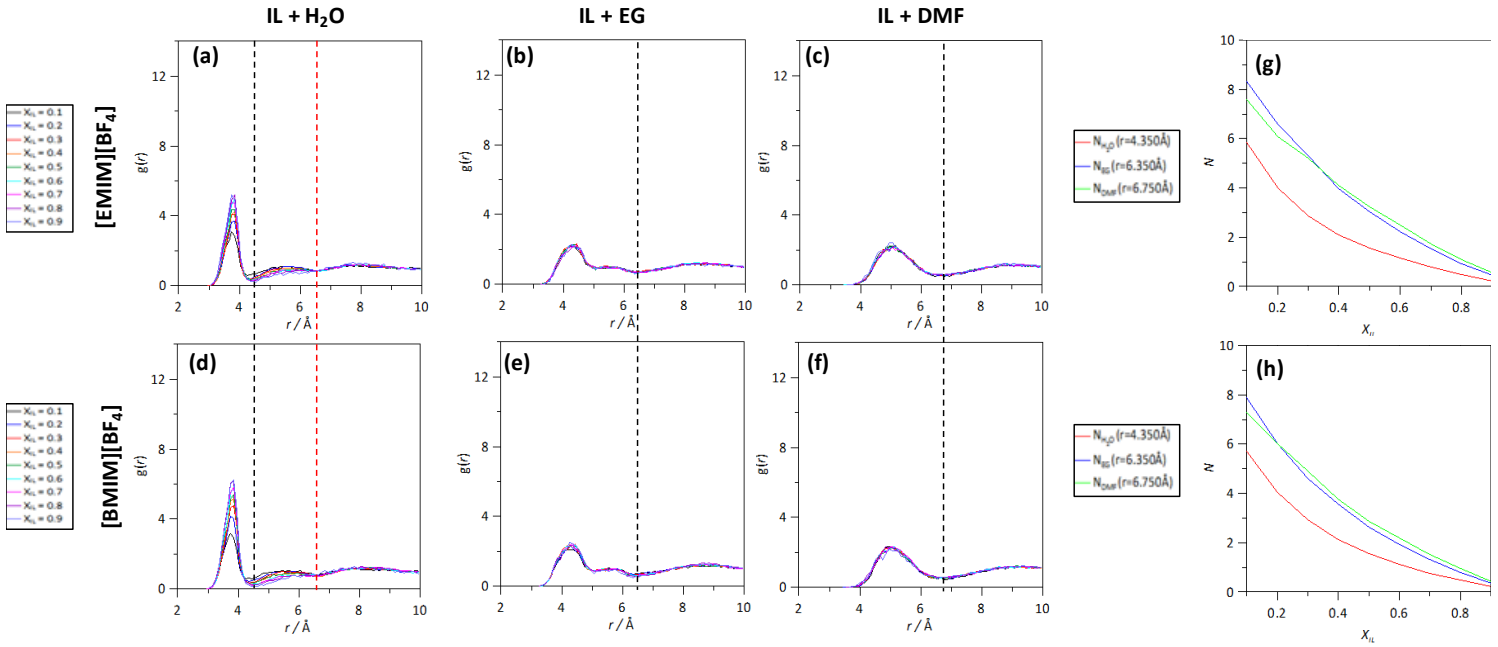


**Fig. 8.**

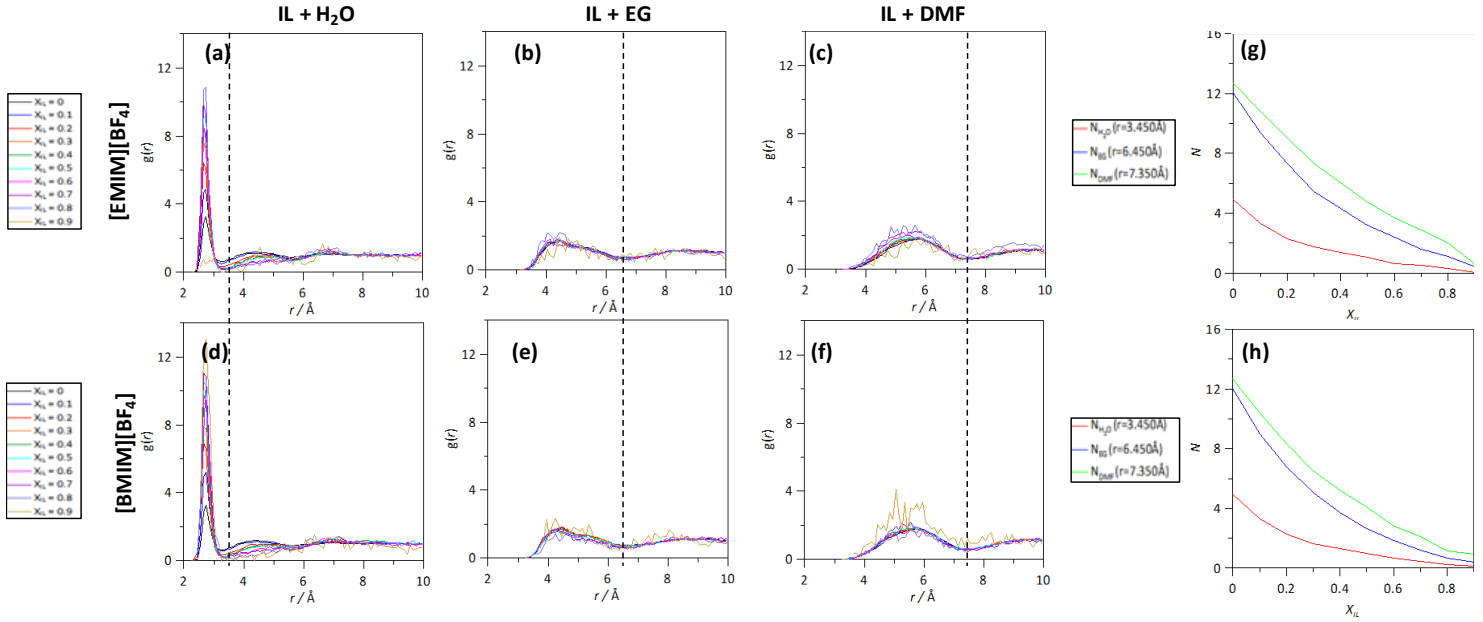


**Fig. 9.**

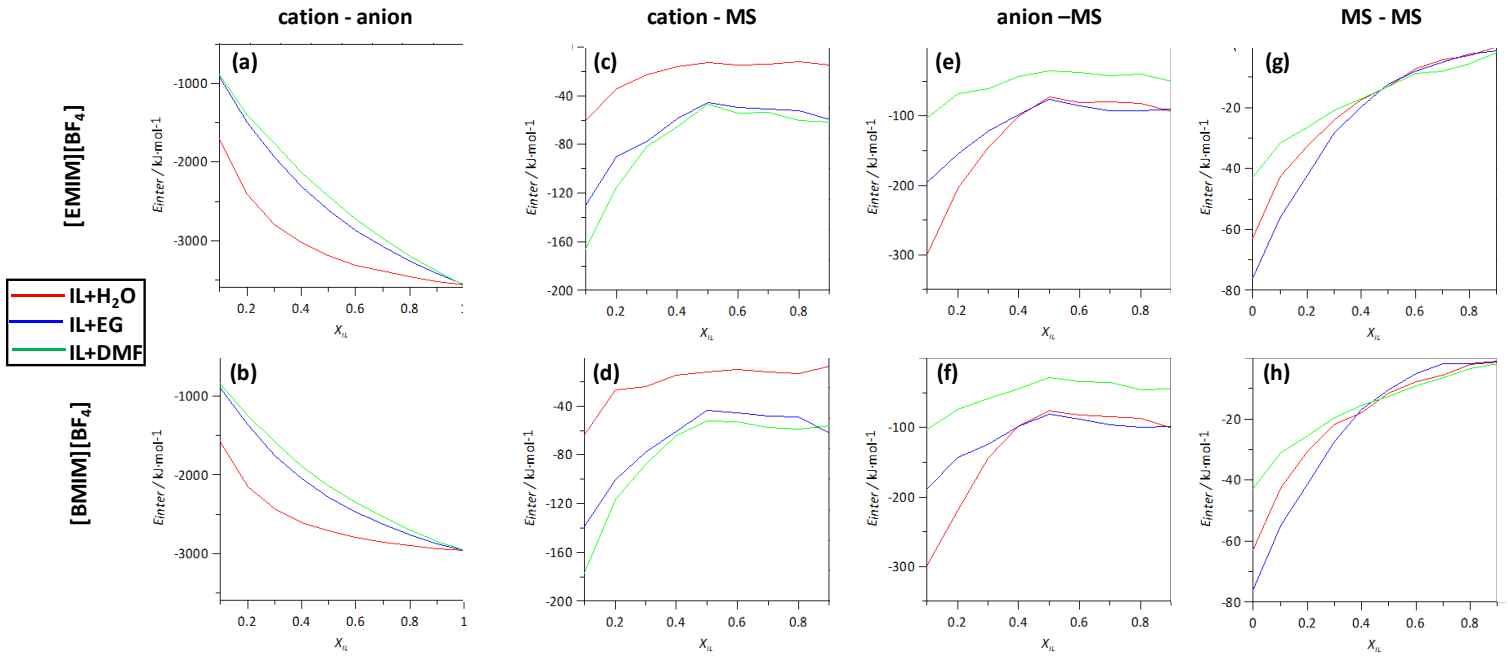


**Fig. 10.**

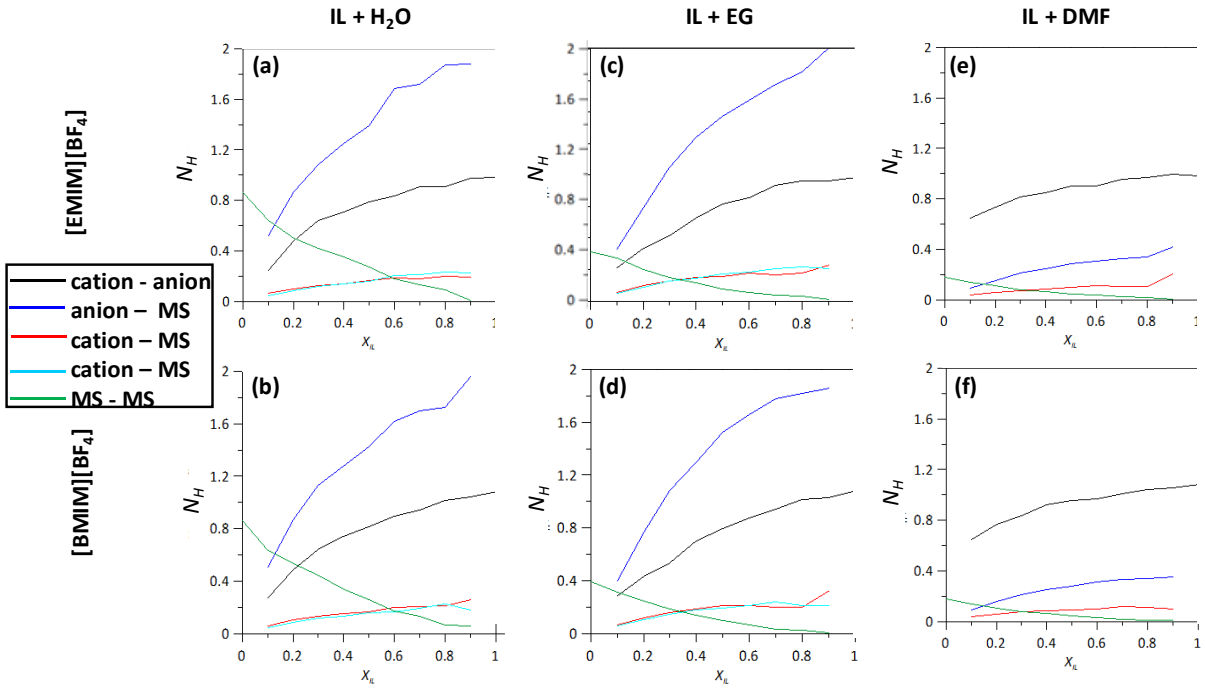


**Fig. 11.**

Highlights

- Ionic liquid mixtures.
- Protic organic solvents
- Physicochemical and theoretical study.
- Quantum chemistry and molecular dynamics.
- Intermolecular forces.